Dust and Biological Aerosols from the Sahara and Asia Influence Precipitation in the Western U.S.

Jessie M. Creamean,[1]*† Kaitlyn J. Suski,[1]* Daniel Rosenfeld,[2] Alberto Cazorla,[1] Paul J. DeMott,[3] Ryan C. Sullivan,[4] Allen B. White,[5] F. Martin Ralph,[5,6] Patrick Minnis,[7] Jennifer M. Comstock,[8] Jason M. Tomlinson,[8] Kimberly A. Prather[1,6]‡

Winter storms in California's Sierra Nevada increase seasonal snowpack and provide critical water resources and hydropower for the state. Thus, the mechanisms influencing precipitation in this region have been the subject of research for decades. Previous studies suggest Asian dust enhances cloud ice and precipitation, whereas few studies consider biological aerosols as an important global source of ice nuclei (IN). Here, we show that dust and biological aerosols transported from as far as the Sahara were present in glaciated high-altitude clouds coincident with elevated IN concentrations and ice-induced precipitation. This study presents the first direct cloud and precipitation measurements showing that Saharan and Asian dust and biological aerosols probably serve as IN and play an important role in orographic precipitation processes over the western United States.

Aerosols can modify cloud microphysical properties, including droplet size and water phase, and thus can alter precipitation efficiency (*1*). In particular, dust aerosols, which originate from various deserts around the world (*2*), have been shown to serve as effective ice nuclei (IN) and potentially enhance precipitation in mixed-phase clouds (*3*). IN are atmospheric particles that catalyze the freezing of supercooled cloud droplets, producing ice crystals that would not form otherwise at warmer, mixed-phase cloud temperatures (*4*). Some types of biological aerosols such as bacteria have also been shown to serve as effective IN at relatively warm temperatures (*5*); however, recent modeling studies have concluded that they are of minor importance to global IN concentrations and precipitation processes (*6*). Biological aerosols (such as bacteria), can be co-lofted and transported with dust (*7*). When lofted to high altitudes (~≥5000 m), dust and biological aerosols can travel long distances. For example, Uno *et al.* showed that dust from the Taklimakan desert in China circled the globe within 13 days (*8*). Intercontinental transport of dust from Asia is well documented (*9*–*12*), whereas few have reported trans-Pacific transport from North Africa (*13*, *14*). Modeling studies have shown that both Asian and African dust influence ice formation in mixed-phase clouds (*15*, *16*). Small amounts of dust can be lofted into the free troposphere from the Taklimakan as early as February, with maximum concentrations detected between April and May. Much of the Gobi desert is frozen in the winter months, but it can represent a substantial Asian dust source in response to strong winter storms from Siberia (*3*). Dust is lofted from the Sahara year round, so this source region has the potential to affect ice formation in clouds throughout the year (*3*).

IN concentrations are generally low (~1 in every 10^5 aerosol particles in the free troposphere at –20°C) (*17*), highly variable, and strongly dependent on the chemical composition of the aerosols present within a particular cloud (*18*). At mixed-phase cloud temperatures (above roughly –36°C), IN are necessary for ice formation. Ice crystals grow diffusionally at the expense of liquid droplets (*19*) and can gain mass through accretion of supercooled liquid droplets or aggregation with other crystals to form graupel or snow (*20*, *21*). Freezing of cloud droplets induced by IN produces a mixed-phase cloud that initiates precipitation more rapidly than does a supercooled, liquid-only cloud because of the faster growth rate of ice particles versus droplets (*22*). The presence, absence, and abundance of IN can thus affect the intensity and spatial distribution of precipitation events. The efficiency of ice and precipitation processes has serious ramifications for mountainous regions such as the California Sierra Nevada, where snowpack supplies copious amounts of water to reservoirs (*23*). Hence, cloud-seeding experiments have been conducted in the Sierra Nevada since 1948 as a possible means of increasing precipitation (*24*, *25*). It has been suggested that over 50% of precipitation globally is initiated in the ice phase [such as in (*26*)]. Therefore, identifying the sources of IN within clouds and the mechanisms by which they influence precipitation processes is critical for future water and energy.

Analysis of precipitation samples in combination with storm meteorology can provide insight into IN effects on orographic precipitation. For example, Ault *et al.* observed insoluble residues in precipitation samples collected in the Sierra Nevada, which were hypothesized to be Asian dust (*1*). There are two key unresolved questions from the Ault *et al.* study: (i) Do the insoluble precipitation residues reflect the composition of the IN that initially nucleated cloud ice? (ii) What role does dust play in affecting cloud microphysics and precipitation? Further evidence from Pratt *et al.* provided aircraft measurements of dust and biological residues colocated with ice in clouds over Wyoming, but this was a limited data set, with no emphasis linking observations with precipitation (*27*). Here, we present results building on those from Ault *et al.* and Pratt *et al.* using a combination of both ground-based precipitation and aircraft in situ cloud measurements in California throughout the 2011 winter. Our results indicate a relationship between dust and biological aerosols detected in in situ cloud residues in distinct mid-level ice layers, residues in precipitation collected at the ground, and long-range transport of dust and biological aerosols from Asia, the Middle East, and the Sahara. Combined, these results strongly suggest dust and biological aerosols affected ice formation in mid-level clouds where precipitation processes were initiated.

The CalWater field campaign was designed to directly address aerosol impacts on clouds and precipitation in the Sierra Nevada during three consecutive winter seasons (2009 to 2011). Measurements from a remote ground site at California's Sugar Pine Dam [SPD, 39°07′42.80″N, 120°48′04.90″W; 1064 m mean sea level (MSL)] included aerosol and meteorological instrumentation from 2009 to 2011. The same technique used by Pratt *et al.* (*27*) and Ault *et al.* (*1*)—aerosol time-of-flight mass spectrometry (ATOFMS) (*28*)—was used to determine the chemical composition of resuspended insoluble precipitation residues collected at SPD from 30 January to 8 March 2011. S-band profiling radar (S-PROF) provided bulk microphysical information using vertical profiles of hydrometeor fall velocity and radar reflectivity (*29*). Precipitation processes included warm rain, which started as liquid; cold rain, which started as ice and melted during descent; and snow/graupel/hail when surface temperatures were low (*30*). Precipitation that starts in the ice phase—snow/graupel/hail and cold rain—

[1]Department of Chemistry and Biochemistry, University of California, San Diego (UCSD), La Jolla, CA 92093, USA. [2]Institute of Earth Sciences, Hebrew University of Jerusalem, Jerusalem 91904, Israel. [3]Department of Atmospheric Science, Colorado State University, Fort Collins, CO 80523, USA. [4]Center for Atmospheric Particle Studies, Carnegie Mellon University, Pittsburgh, PA 15213, USA. [5]Physical Sciences Division (PSD), National Oceanic and Atmospheric Administration (NOAA)/Earth System Research Laboratory (ESRL), Boulder, CO 80305, USA. [6]Scripps Institution of Oceanography (SIO), University of California, San Diego, La Jolla, CA 92093, USA. [7]NASA Langley Research Center, Hampton, VA 23681, USA. [8]Atmospheric Sciences and Global Change Division, Pacific Northwest National Laboratory (PNNL), Richland, WA 99352, USA.

*These authors contributed equally to this work.
†Present address: Physical Sciences Division (PSD), National Oceanic and Atmospheric Administration (NOAA)/Earth System Research Laboratory (ESRL), Boulder, CO 80305, USA.
‡Corresponding author. E-mail: kprather@ucsd.edu

Downloaded from http://science.sciencemag.org/ on January 21, 2017

is termed "ice-induced precipitation." S-PROF time-height cross sections during the times for all 11 of the precipitation sampling periods are shown in fig. S1.

During all of the 2011 storms, dust and biological residues were frequently present in the precipitation, comprising up to 99% of the total insoluble residues per sample. The percentage of dust plus biological residues (%Dust+Bio), median cloud top temperature (°C), relative amount of cloud ice (%Ice), and percentages of different precipitation processes during each sample collection date in 2011 are shown in Fig. 1. Dust and biological residue percentages were combined for the precipitation analysis because chemical markers for each type were often observed within the same individual residue owing to the precipitation collection and aerosolization processes (fig. S2 and supplementary text). Ice-induced precipitation comprised 74% of the total precipitation that fell at SPD, whereas warm rain comprised only 10% (the remaining 16% was unclassified). The highest %Dust+Bio in precipitation samples occurred during storms that contained a higher percentage of ice-induced precipitation (such as 30 January, 16 to 19 February, and 24 to 26 February). During these storms, surface temperatures were sufficiently low (table S1), enabling snow/graupel/hail to reach the surface. During the storms from 14 to 16 February, 1 to 3 March, and 5 to 7 March, surface temperatures were higher, resulting in more rain than ice at the surface. Further, more warm rain coincided with lower %Dust+Bio during these time periods. For the five samples in which >50% of precipitation fell as snow/graupel/hail, the average %Dust+Bio was 90%, whereas for the four cases in which >30% of the precipitation occurred as warm rain, the average %Dust+Bio was 69%. One possible explanation could be that a limited amount of dust and biological aerosols were available to serve as IN, leading to less precipitation initiated in the ice phase. Another potential explanation is that the thermodynamic and dynamic structure of the storm produced shallower clouds (fig. S1) with warm rain, which were perhaps unable to reach vertically into the dust plume. Typically, the cloud top temperatures were lower when the %Dust+Bio in precipitation and %Ice in cloud were higher, suggesting that dust and biological aerosols are more efficiently activated and scavenged via ice nucleation at colder temperatures. Both the 1 to 2 March and 2 to 3 March time periods had similar cloud top temperatures (–22°C); however, the %Dust+Bio and %Ice were higher on 1 to 2 March and lower on 2 to 3 March. Thus, this result suggests that the formation of in-cloud ice is not entirely dependent on the cloud temperature alone and that the presence and abundance of IN feeding the clouds is important. Overall, these results suggest that dust and biological aerosols probably served as IN and influenced the precipitation phase in the clouds within colder sectors of the storms, expanding on the precipitation measurements made by Ault *et al*. in 2009. Precipitation residues can provide useful information on the nature of aerosols and cloud seeds; however, because of the caveats involved with analyzing precipitation and correlating ground-based measurements with mid-level cloud processes, in situ aircraft measurements of cloud residues made during CalWater 2011 were critical for gaining further insight into the role of the dust and biological particles in cloud and precipitation processes.

A compact aircraft version of the ATOFMS (*31*) measured in situ cloud droplet and ice crystal residues onboard the G-1 during CalWater. Cloud residue data during each precipitation sampling time period are included in Fig. 1. Discussion regarding the collection of cloud residues and the relative amount of dust and biological residues in the precipitation compared with the cloud residues is provided in the supplementary materials. High percentages of dust and dust mixed with biological cloud residues were observed during the flights on 16 and 25 February, respectively. On 16 February, the cloud residues were rich in aluminosilicate dust (50%), with smaller contributions from dust mixed with biological material ("dust/biological," 16%) and purely biological residues (3%). However, on 25 February, residues were predominantly composed of dust mixed with salt and biological material ("dust/salt/biological," 66%), whereas dust and biological residues represented 9 and 10%, respectively. The precipitation residues were also characterized as more "dustlike" on 16 February and were composed of biological material on 25 February (supplementary text). Although the precipitation residue compositions were not exactly the same as the cloud residues, the similarities between the two suggest that the majority of precipitation residues probably originated from the cloud particles as opposed to being scavenged by precipitation in the air below cloud base. The meteorological conditions were similar during these 2 days and corresponded

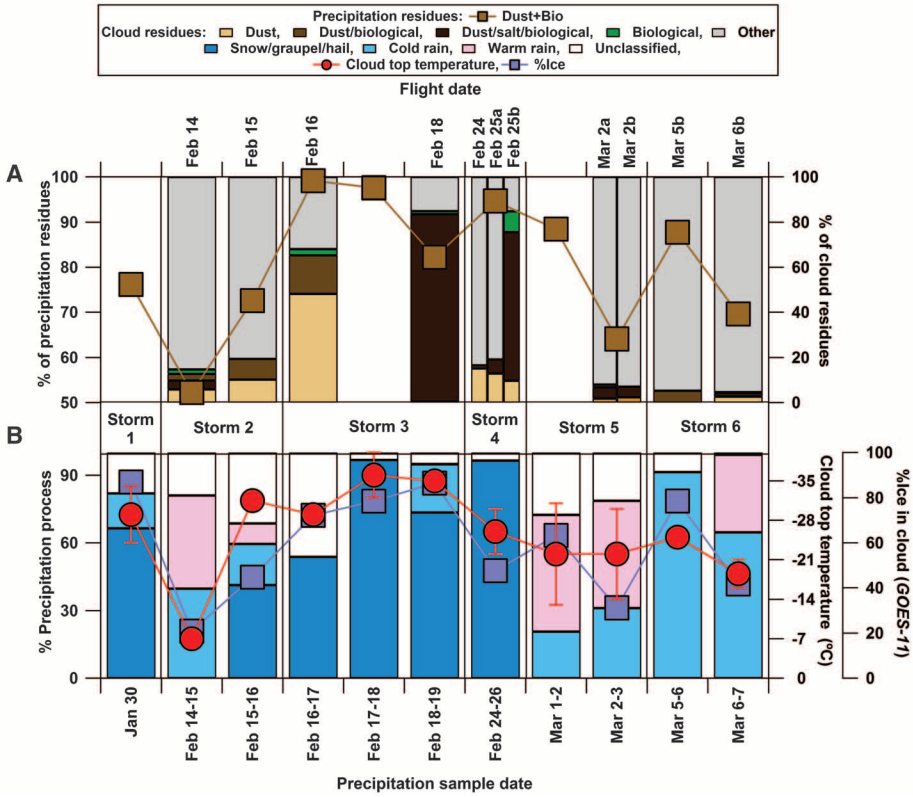

Fig. 1. Precipitation and cloud characteristics during each sample collection date during the 2011 CalWater study at SPD. (**A**) Markers show the percentages of dust and biological precipitation residues combined (Dust+Bio) sampled at the surface at SPD, and bars show the percentages of in-cloud residues sampled on the G-1 aircraft. Sample dates with more than one column of bars for the aircraft data signify more than one flight took place; for instance, three flights were taken 24 to 26 February and two flights were taken 2 to 3 March. (**B**) The percentages of cold rain, snow/graupel/hail, and warm rain per sample (taken from S-PROF radar profiles). Red markers represent the median cloud top temperature (in degrees Celsius) per sample collection date. Error bars are shown for temperature and represent the minimum and maximum of the range. Violet markers represent the average relative amount of the cloud consisting of ice (%Ice) within the 10-km radius over SPD derived from satellite measurements. Storms 1 to 6 are highlighted in order to identify the evolution of cloud and precipitation residues, cloud top temperature, %Ice, and precipitation processes over the course of the storms.

Downloaded from http://science.sciencemag.org/ on January 21, 2017

to the passing of a cold front (supplementary text). The passing of these cold fronts probably enabled the transport of dust and biological aerosols into the region, as suggested by previous studies (*1*). However, if IN were hypothetically absent in these cold air masses, supercooled cloud droplets would remain as liquid instead of forming ice crystals, as as shown by Rosenfeld *et al.* (*32*) and described here. On days without these meteorological conditions, we observed only minor fractions of dust and biological particles in cloud residues (fig. S4), showing that dust and biological particles are not always present. Additionally, estimated dust concentrations detected between 3000 and 6000 m are provided and discussed in the supplementary materials to show that the variability of dust concentrations can range over an order of magnitude during flights. This strongly supports the concept proposed here that ice formation depends not only on the meteorological conditions but also on the availability of effective IN, such as certain mineral dusts and biological particles.

In order to investigate the impact of dust and biological particles on cloud properties during the storms on 16 to 19 February and 24 to 26 February, we examined data from the flights corresponding to these storms in more detail. Shown in Fig. 2 are the number of individual cloud residues measured by A-ATOFMS for the 16 February ascent (Fig. 2A) and 16 February descent (Fig. 2B) flight segments (flight tracks are available in the supplementary materials). The 25 February ascent and descent are shown in fig. S8. Flights on 16 and 25 February are separated into the ascent and descent because of changing dynamics (supplementary text). The early mornings on 16 and 25 February included prefrontal periods with an atmospheric river (narrow band of water vapor transported from subtropical oceanic regions) and terrain-parallel blocked flows (supplementary text), which introduced moist marine air masses into deep clouds over the Sierra Nevada (fig. S1). In the afternoon during the flights on 16 and 25 February, cold postfrontal conditions with lower-level convective clouds and mid-level orographic clouds were present. Liquid water content (LWC), the mass concentration of liquid in a cloud, was measured with a cloud droplet probe (CDP). IN concentrations (IN per liter of air) were measured with a continuous flow diffusion chamber (CFDC) (*17*). Cloud ice fraction was calculated by using liquid and total water content measured with the WCM-2000 (SEA, Mansfield Center, Connecticut). Details of the calculation are available in the supplementary materials.

During the ascent to high altitudes on 16 February, the lower-level convective clouds (≤3500 m) were pristine marine clouds that contained predominately sea salt residues and few dust particles (Fig. 2A). Correspondingly, the IN concentrations were low (0 to a maximum of 0.15 ± 0.2 liter^{-1} in a temperature range from –18.4 to –18.9°C). These measurements were consistent with little to no ice in-cloud as evidenced by a low cloud ice fraction (0 to 0.4) and high LWC (up to ~1 g/m^3). The nearly ice-free, supercooled cloud reached temperatures down to –21°C. The presence of liquid water and lack of large amounts of ice was consistent with very few IN active in this region of the cloud. The IN concentrations in the mid-level orographic clouds (4000 to 6000 m) could be determined with greater certainty at 0.16 ± 0.06 liter^{-1} measured at –18.8°C, whereas the cloud top temperature reached –35°C and contained ice along with supercooled water of <0.1 g/m^3. In addition, a spike in dust and dust/biological residues was observed between 4400 and 5500 m in these mid-level clouds. Transmission electron microscopy (TEM) analysis showed that 88% of IN-activated aerosol in the CFDC was of dust and biological origin (53% dust, 26% dust/salt/biological, and 9% biological)—thus confirming the dominance of dust and biological cloud residues observed by the A-ATOFMS, as discussed above. However, above 5500 m we observed less dust and biological residues coincident with supercooled liquid water at temperatures as low as –35°C, thus showing a distinct layer of dust and biological aerosols played a role in forming the ice-enriched layer at lower altitudes and warmer temperatures. During the

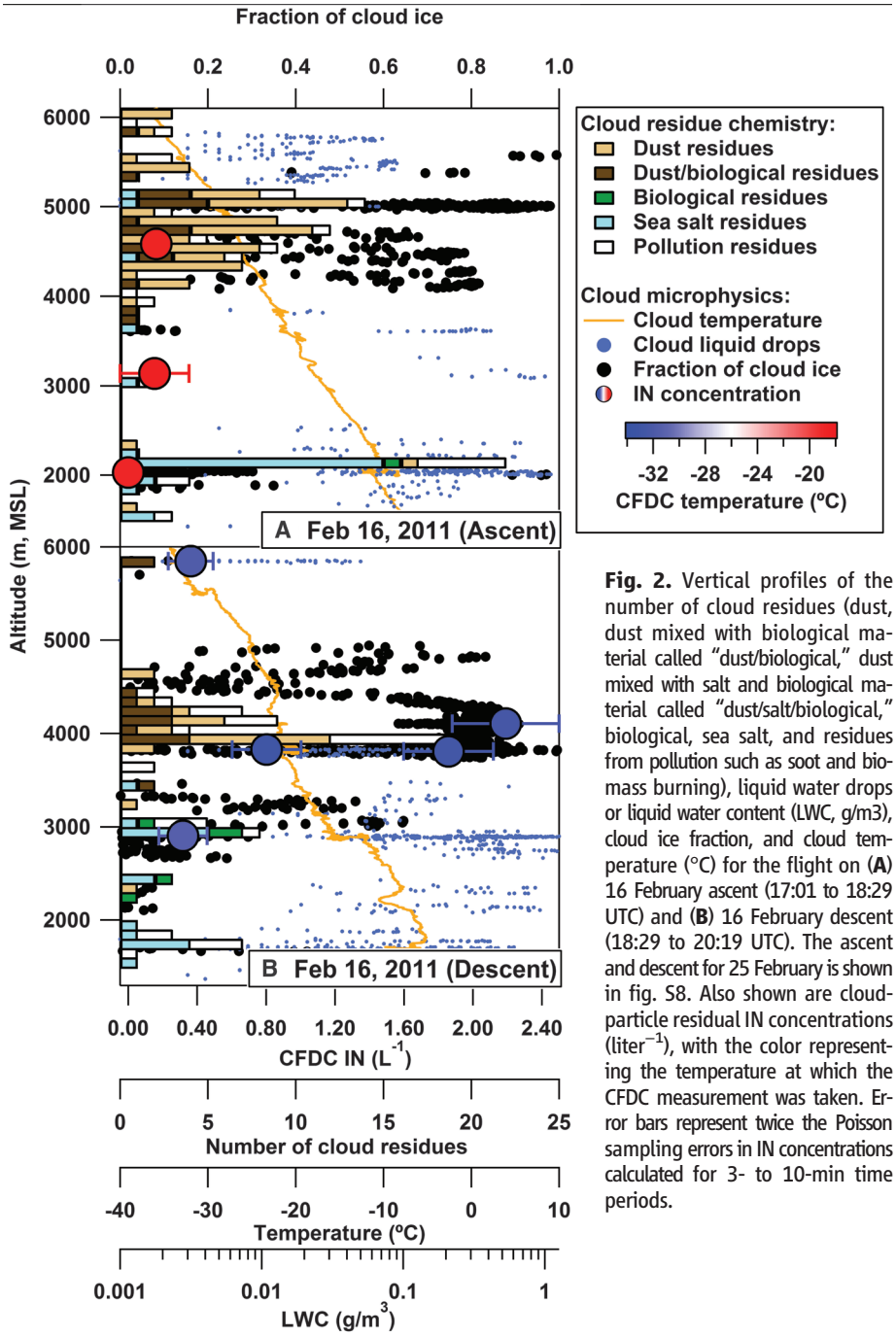

Fig. 2. Vertical profiles of the number of cloud residues (dust, dust mixed with biological material called "dust/biological," dust mixed with salt and biological material called "dust/salt/biological," biological, sea salt, and residues from pollution such as soot and biomass burning), liquid water drops or liquid water content (LWC, g/m3), cloud ice fraction, and cloud temperature (°C) for the flight on (**A**) 16 February ascent (17:01 to 18:29 UTC) and (**B**) 16 February descent (18:29 to 20:19 UTC). The ascent and descent for 25 February is shown in fig. S8. Also shown are cloud-particle residual IN concentrations (liter^{-1}), with the color representing the temperature at which the CFDC measurement was taken. Error bars represent twice the Poisson sampling errors in IN concentrations calculated for 3- to 10-min time periods.

Downloaded from http://science.sciencemag.org/ on January 21, 2017

descent back down to lower altitudes (Fig. 2B), dust and dust/biological cloud residues were detected at several altitudes but were most abundant between 3500 and 4500 m, where the highest ice fractions were observed (up to 1). IN concentrations measured at a lower CFDC processing temperature of –32 ± 0.5°C trended with the abundance of the dust and biological residues, reaching 2.2 ± 0.3 liter^{-1} between 4000 and 4500 m. The large increase in IN concentrations measured in dust layers at –32°C on the descent as compared with those at –18.4° to –18.8°C on the ascent suggests that the dust was IN-active within the intermediate temperature range. The co-location of these specific residues with ice crystals and higher IN concentrations suggest dust and biological aerosols served as IN in these mid-level clouds.

On 25 February, the meteorological and cloud conditions were similar to those of 16 February. However, dust/salt/biological aerosols as opposed to pure dust on 16 February were co-located with ice, particularly around 2700 and 3900 m. The residues were separated into two distinct layers, as shown in fig. S8A: a lower layer from 1400 to 3100 m and an upper layer from 3800 to 4000 m. IN concentrations reached 0.39 ± 0.2 liter^{-1} measured at –25.0°C in the upper layer, whereas in the lower layer, maximum IN concentrations of 0.51 ± 0.24 liter^{-1} were measured at –25.3°C; the CFDC temperatures were appropriate for the upper layer (–26° to –20°C) but colder than cloud temperatures in the lower layer (–17° to –10°C). The mixed nature of these particles makes it difficult to extract which component (dust or biological) enabled the ice formation. The observations on 16 and 25 February bracket the activation temperatures of the dust and biological particles between –18° and –32°C, with most of the activity occurring below –25°C. This is in agreement with previous laboratory studies, showing that many mineral dusts are more IN-active below ~–20°C, whereas biological particles such as spores become active at ~–28°C (*32*), as well as with satellite observations of Asian desert dust glaciating cloud tops at –22°C on average (*3*).

On 25 February, the mid-level cloud contained supercooled cloud water of up to 0.3 g/m^3, with some ice crystals that rimed into graupel at lower levels (supplementary text), suggesting that the ice was formed in the mid-level cloud and fell into the lower-level cloud while riming and depleting the cloud water. These results, along with the results on 16 February, are indicative of the seeder-feeder mechanism (*33*), which has been documented previously in the Sierra Nevada (*34*) as well as in other mountain regions including those in Colorado, Oregon, Washington, Arizona, and central Europe (*35*–*38*). These data suggest that particles with biological components, in addition to dust, play a role in ice formation in the orographic clouds in the Sierra Nevada and contribute to the efficiency of the seeder-feeder mechanism. Previous studies have shown that a graupel particle grows much faster than does a supercooled raindrop of the same mass in the same convective cloud (*22*). Therefore, seeder-feeder is an efficient precipitation mechanism, especially when the accreted drops are large (*39*). Satellite observations have suggested the possibility of dust glaciating high-altitude clouds (*40*); however, there have not been any in situ measurements of dust in clouds over the Sierra Nevada before this study. When urban pollution aerosols are incorporated into clouds, precipitation processes are often less efficient, and suppression of both warm and mixed-phase precipitation has been shown via satellite (*41*, *42*). Our results show that the presence of dust and biological particles feeding deeper and colder orographic cloud levels appears to have the opposite effect—accelerating the efficiency of the precipitation-forming processes, especially in situations in which cloud layers are decoupled from the boundary layer, likely because of the presence of terrain-parallel blocked flow (supplementary text). To address this, future studies

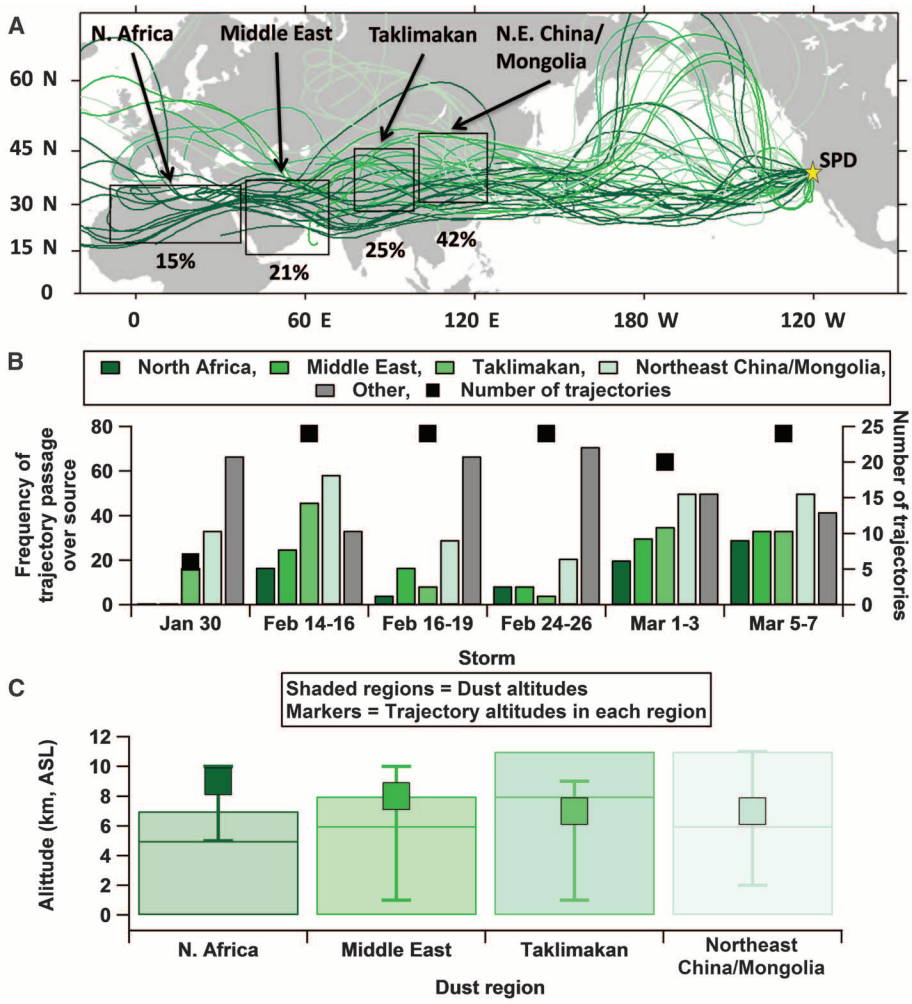

Fig. 3. Dust source analysis including (**A**) 10-day back trajectories ending at cloud top heights over SPD during storms in 2011, with the boxes highlighting the four dust source regions. Trajectories are colored according to which dust region they traveled over, including the Sahara (separated into North Africa and the Middle East) and East Asia (separated into the Taklimakan desert and Northeast China/Mongolia). Storms were investigated in order to achieve statistical significance (more trajectories per time period). The percentages under each box represent the frequency that the trajectories passed through each arid region. (**B**) The frequency with which 10-day back trajectories passed over the dust regions defined in (A) in addition to other regions (nondust origin). The four shades of green represent the four different dust regions. The total number of trajectories analyzed per storm is also provided. (**C**) The average altitudes of trajectories that passed through each region and dust layer heights determined by using NAAPS analysis time-height sections at Sedeboker (North Africa), Solar Village (Middle East), Yinchuan (site nearest to the Taklimakan), and Beijing (Northeast China/Mongolia) for the time periods studied. A map of the sites and examples of the time-height sections are shown in fig. S11. Data originate from time periods that include back trajectory end points shown in fig. S13. The middle line of the shaded regions represents the average maximum height of the dust layers in each region from NAAPS analysis. The error bars show the minimum and maximum altitudes for the trajectory end points and dust layers.

Downloaded from http://science.sciencemag.org/ on January 21, 2017

should be designed to observe both influences, boundary-layer and upper-level aerosols, as well as associated meteorological conditions.

The co-location of dust and biological aerosols with IN and ice in clouds, in addition to the abundance of dust and biological residues observed on days with more ice-induced precipitation during CalWater, leads to a question of the origin of the dust and biological aerosols. Ault *et al.* suggested Asian dust influenced snowfall during only one storm in 2009 (*9*); however, we present here six storms with influences from Asia and the Sahara. Local sources of dust and biological aerosols were probably minor contributors to the precipitation residues (supplementary text). Ten-day air mass backward trajectories are shown in Fig. 3A, calculated with HYSPLIT (*43*) ending at SPD during the storms shown in Fig. 1. Meyers *et al*. suggest that ice nucleation occurs at the tops of orographic clouds (*34*), and thus trajectories were calculated to end at cloud top heights between 2000 and 10,000 m MSL over SPD by using data from the 11th Geostationary Operational Environmental Satellite (GOES-11) averaged every 3 hours during storms. The boxes highlight major dust regions (*2*). Based on previous studies [such as (*44*)], some biological aerosols were probably co-lofted from arid regions and transported with the dust, although other sources of biological material such as the ocean and local sources could also contribute. The frequency of trajectories that traveled over each dust region during each storm is shown in Fig. 3B. Trajectories that originated from over North Africa frequently traveled over the other dust regions on the way to the United States, suggesting that these air masses contained a mixture of dust from the various source regions. Further, wet and dry deposition of the dust and biological aerosols could contribute to loss during transport from the more distant sources (Africa). The dust source frequencies show that the storms were predominantly affected by Asia; however, the end of the study was additionally influenced by North Africa and the Middle East (15 and 21% of the time, respectively). Not only did the air masses travel over the various dust regions, the air intersected dust layers (Fig. 3C). Using time-height cross sections of dust concentrations from the Navy Aerosol Analysis and Prediction System (NAAPS, www.nrlmry.navy.mil/aerosol), we estimated the maximum height of dust layers at sites within or near each dust region on days during which the trajectories traveled over the boxes. The height of trajectories that passed through each region typically fell within the height of the dust layers (Fig. 3C). Although transport within the dust layers was infrequent over North Africa, Saharan dust was probably picked up over the Middle East, where trajectories, on average, skimmed the top of the layer. Overall, trajectories traveled through dust layers 6, 23, 73, and 45% of the time in North Africa, the Middle East, the Taklimakan, and Northeast China/Mongolia, respectively (fig. S13).

Further evidence that dust was present along the complete trajectory was obtained by using Cloud-Aerosol Lidar and Infrared Pathfinder Satellite Observation (CALIPSO) satellite data of aerosol subtypes. In combination with NAAPS, CALIPSO provides a method to track dust as it is transported from the source across the Pacific Ocean to SPD (fig. S14). NAAPS-modeled aerosol optical depth (AOD) of dust is shown in Fig. 4, in addition to locations where CALIPSO imagery transected the trajectories for 16 and 25 February. These two days represent the storms in which the highest %Dust+Bio was present in the precipitation (93 and 95% on average during 16 to 19 February and 24 to 26 February). The trajectory ending on 16 February started 10 days earlier over the Atlantic Ocean and proceeded to travel north of the Saharan dust layer. Before reaching China, the air mass contained little dust according to CALIPSO imagery (Fig. 4A, the "No Dust" circle). Once the air mass reached Northeast China/Mongolia, it picked up fresh dust and traveled across the Pacific Ocean to SPD. In contrast, the trajectory ending on 25 February started 10 days back over Oman, where an abundance of fresh dust was present. The air mass continued to travel over southern China, where it probably picked up more dust from the Asian sources. The CALIPSO imagery following the trajectory over the Pacific Ocean shows both fresh and polluted dust. Combined analysis of air mass back trajectories, NAAPS, and CALIPSO imagery provides evidence of lofted dust being transported across the Pacific Ocean and shows the probable sources of IN that influence precipitation processes in the Sierra Nevada. Conventionally, dust from the Sahara has been shown to travel west over the Atlantic Ocean from Africa to South America; however, here we show African dust traveling east across the Pacific and into the United States at higher altitudes.

We present a direct link between long-range transported dust and biological aerosols affecting cloud ice formation and precipitation processes in the Sierra Nevada. As summarized in Fig. 5, long-range transport of the dust and biological aerosols is shown to be an important mechanism for introducing IN into mid-level clouds and enhancing precipitation formation via seeder-feeder in the Sierra Nevada. Developing this whole conceptual picture requires combining evidence from multiple measurements, including (i) ground-based precipitation chemistry, (ii) satellite data showing dust activity and transport, (iii) aircraft in situ cloud microphysics and residual aerosol composition, (iv) detailed meteorology at the ground level as well as within the clouds, and (v) out-of-cloud aerosol measurements (>0.6 μm). This study is the first to show dust originating from further west than Asia plays a role in clouds and precipitation processes over the western United States. Dust and biological aerosols measured as insoluble residues in precipitation samples corresponded to periods with more ice-induced precipitation. In situ aircraft measurements of the same storm systems confirmed that the dust and biological

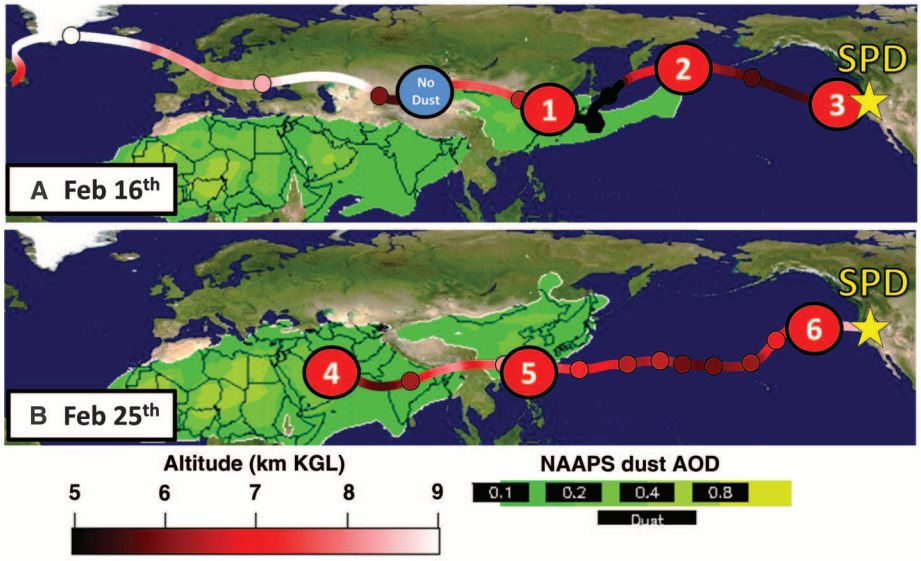

Fig. 4. Dust tracking for days during the (**A**) 14 to 16 February and (**B**) 24 to 26 February storms. The 10-day air mass back trajectories ended at cloud-top heights over SPD (shown by the star) on 16 February (7390 m MSL) and 25 February (9340 m MSL). Within each trajectory, the color scale represents the altitude of each hourly end point, whereas the circles show each end point at 00:00; each marker represents 1 day back. The last 2 days from the trajectory ending on 16 February are not shown. The circled numbers mark the locations where dust was present along these trajectories determined by using CALIPSO imagery (fig. S14). The green overlays represents dust AOD from 0.1 to 0.8 modeled by NAAPS. The dust AOD overlays are composites of the 10 days during each trajectory: (A) 6 to 16 February and (B) 15 to 25 February.

Downloaded from http://science.sciencemag.org/ on January 21, 2017

precipitation residues were co-located in a distinct cloud layer, with higher IN concentrations and larger fractions of ice relative to supercooled liquid. Many factors contribute to the type and quantity of precipitation, including dynamics, meteorological forcings, and transport conditions; however, our results suggest that dust and biological particles play a key role in ice formation and potentially precipitation initiation by causing glaciation of mid-level clouds. Further, our results also suggest that biological particles may play a larger role than modeling studies suggest, which indicates further studies are needed on the surface emission rates, oceanic fluxes, and IN efficiency of biological aerosols, of biological aerosols, especially when mixed with other species. In situ cloud measurements such as these provide critical insights into the key chemical species involved in the formation of ice in clouds; however, controlled laboratory studies are needed to better understand the mechanisms involved as well as sort out critical chemical details, such as whether metals, minerals, biological material, or some combination control the initial ice formation process.

Before this study, most studies had focused on modeling the impacts of regional aerosol pollution sources on precipitation. Our results demonstrate the potentially critical impact of intercontinental transport of natural aerosols on precipitation-formation processes. Further, these findings motivate the challenging study of quantifying aerosol effects on not only the initial cloud phase and formation of precipitation but also the intensity and location of precipitation. Such studies must also quantify the role of non–aerosol-related meteorological forcings of orographic precipitation. Because of the ubiquity of dust and biological particles such as bacteria in the atmosphere, these findings have global importance. Furthermore, the implications for future water and energy resources from hydropower become even more substantial when considering the possible increase in Aeolian dust as a result of a warming climate and land-use changes.

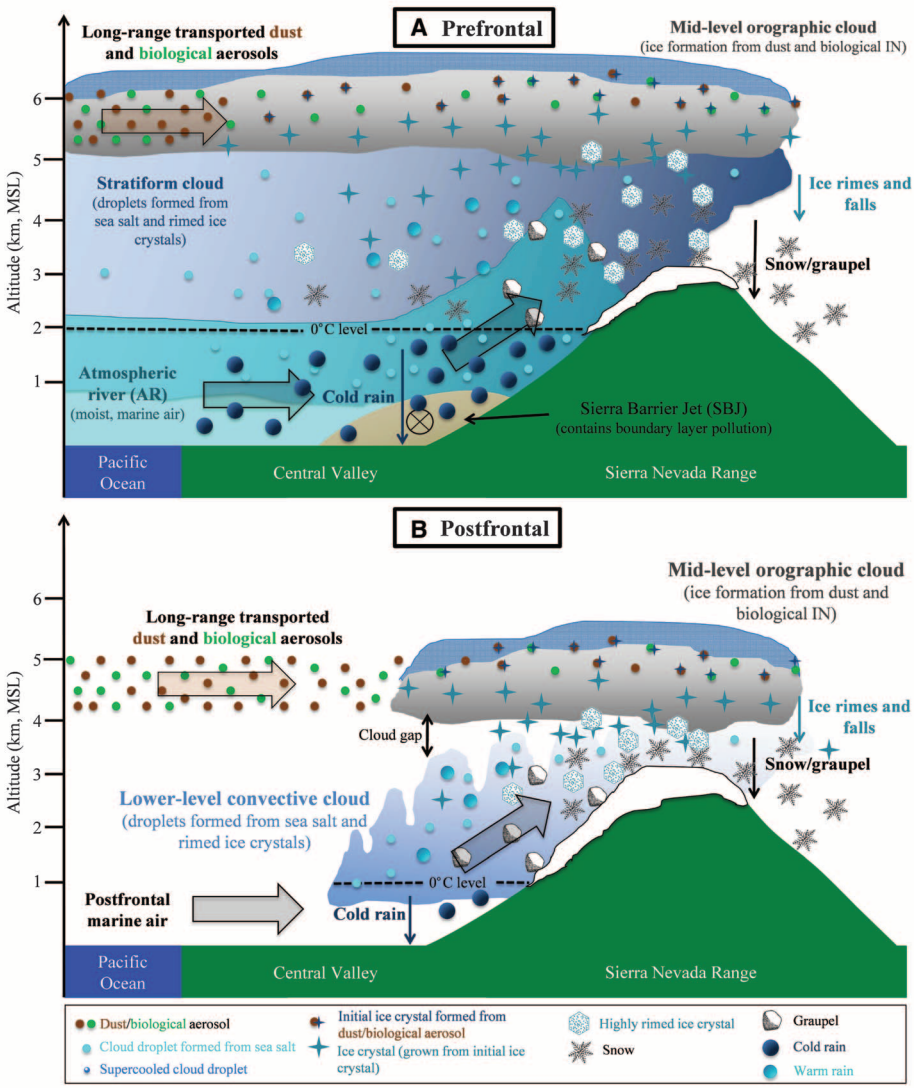

Fig. 5. Conceptual model summarizing results from (**A**) prefrontal and (**B**) postfrontal conditions presented here. Prefrontal conditions corresponded to a deep continuous cloud layer, atmospheric river (AR), and terrain-parallel blocked flow [Sierra Barrier Jet (SBJ)], which shifted to two cloud layers, and the disappearance of the AR and blocked flow during the postfrontal conditions. Dust and biological aerosols are long-range transported and form ice in mid-level orographic clouds. The ice becomes rimed by supercooled drops and falls into lower-level convective clouds formed in pristine, marine air masses. Thus, precipitation is formed via the seeder-feeder mechanism.

References and Notes

1. M. O. Andreae, D. Rosenfeld, *Earth Sci. Rev.* **89**, 13 (2008).
2. J. M. Prospero, P. Ginoux, O. Torres, S. E. Nicholson, T. E. Gill, *Rev. Geophys.* **40**, 1002 (2002).
3. D. Rosenfeld *et al.*, *Geophys. Res. Lett.* **38**, L21804 (2011).
4. K. Isono, M. Komabayasi, A. Ono, *J. Meteorol. Soc. Jpn.* **37**, 211 (1959).
5. C. E. Morris, D. G. Georgakopoulos, D. C. Sands, *J. Phys. IV* **121**, 87 (2004).
6. C. Hoose, J. E. Kristjansson, S. M. Burrows, *Environ. Res. Lett.* **5**, 024009 (2010).
7. K. Hara, D. Z. Zhang, *Atmos. Environ.* **47**, 20 (2012).
8. I. Uno *et al.*, *Nat. Geosci.* **2**, 557 (2009).
9. A. P. Ault *et al.*, *J. Geophys. Res.* **116**, (D16), D16205 (2011).
10. R. B. Husar *et al.*, *J. Geophys. Res.* **106**, (D16), 18317 (2001).
11. I. Uno *et al.*, *Atmos. Chem. Phys.* **11**, 7333 (2011).
12. J. M. Sun, M. Y. Zhang, T. S. Liu, *J. Geophys. Res.* **106**, (D10), 10325 (2001).
13. I. G. McKendry *et al.*, *J. Geophys. Res.* **112**, (D1), D01103 (2007).
14. S.-C. Hsu *et al.*, *Geophys. Res. Lett.* **39**, L12804 (2012).
15. A. Wiacek, T. Peter, U. Lohmann, *Atmos. Chem. Phys.* **10**, 8649 (2010).
16. P. J. DeMott *et al.*, *Geophys. Res. Lett.* **30**, 1732 (2003).
17. D. C. Rogers, P. J. DeMott, S. M. Kreidenweis, Y. L. Chen, *J. Atmos. Ocean. Technol.* **18**, 725 (2001).
18. P. J. DeMott *et al.*, *Proc. Natl. Acad. Sci. U.S.A.* **107**, 11217 (2010).
19. A. Korolev, *J. Atmos. Sci.* **64**, 3372 (2007).
20. C. L. Hosler, D. C. Jensen, L. Goldshlak, *J. Meteorol.* **14**, 415 (1957).
21. R. A. Houze, *Cloud Dynamics* (Academic Press, San Diego, USA, 1993).
22. M. Pinsky, A. Khain, D. Rosenfeld, A. Pokrovsky, *Atmos. Res.* **49**, 99 (1998).
23. B. Guan, N. P. Molotch, D. E. Waliser, E. J. Fetzer, P. J. Neiman, *Geophys. Res. Lett.* **37**, L20401 (2010).
24. D. W. Reynolds, A. S. Dennis, *Bull. Am. Meteorol. Soc.* **67**, 513 (1986).
25. T. Deshler, D. W. Reynolds, A. W. Huggins, *J. Appl. Meteorol.* **29**, 288 (1990).
26. K. M. Lau, H. T. Wu, *Geophys. Res. Lett.* **30**, 2290 (2003).
27. K. A. Pratt *et al.*, *Nat. Geosci.* **2**, 398 (2009).
28. E. Gard *et al.*, *Anal. Chem.* **69**, 4083 (1997).
29. A. B. White, J. R. Jordan, B. E. Martner, F. M. Ralph, B. W. Bartram, *J. Atmos. Ocean. Technol.* **17**, 1226 (2000).
30. A. B. White, P. J. Neiman, F. M. Ralph, D. E. Kingsmill, P. O. G. Persson, *J. Hydrometeorol.* **4**, 264 (2003).
31. K. A. Pratt *et al.*, *Anal. Chem.* **81**, 1792 (2009).
32. R. Iannone, D. I. Chernoff, A. Pringle, S. T. Martin, A. K. Bertram, *Atmos. Chem. Phys.* **11**, 1191 (2011).
33. T. W. Choularton, S. J. Perry, *Q. J. R. Meteorol. Soc.* **112**, 335 (1986).
34. M. P. Meyers, P. J. Demott, W. R. Cotton, *J. Appl. Meteorol.* **31**, 708 (1992).
35. D. Fowler *et al.*, *Water Air Soil Pollut.* **85**, 2107 (1995).
36. A. J. Dore, M. Sobik, K. Migala, *Atmos. Environ.* **33**, 3301 (1999).

Downloaded from http://science.sciencemag.org/ on January 21, 2017

37. S. M. Saleeby, W. R. Cotton, D. Lowenthal, R. D. Borys, M. A. Wetzel, *J. Appl. Meteorol. Climatol.* **48**, 903 (2009).
38. R. F. Reinking, J. B. Snider, J. L. Coen, *J. Appl. Meteorol.* **39**, 733 (2000).
39. R. D. Borys, D. H. Lowenthal, D. L. Mitchell, *Atmos. Environ.* **34**, 2593 (2000).
40. Y. S. Choi, R. S. Lindzen, C. H. Ho, J. Kim, *Proc. Natl. Acad. Sci. U.S.A.* **107**, 11211 (2010).
41. D. Rosenfeld, *Science* **287**, 1793 (2000).
42. A. Givati, D. Rosenfeld, *J. Appl. Meteorol.* **43**, 1038 (2004).
43. R. R. Draxler and G. D. Rolph, HYSPLIT (HYbrid Single-Particle Lagrangian Integrated Trajectory) Model, NOAA Air Resources Laboratory, Silver Spring, MD (2013); available at http://ready.arl.noaa.gov/HYSPLIT.php.
44. A. G. Hallar *et al.*, *Geophys. Res. Lett.* **38**, L17801 (2011).

Acknowledgments: Funding was provided by the California Energy Commission under contract CEC 500-09-043. D.R. was funded under the Atmospheric System Research (ASR)/U.S. Department of Energy (DOE) program. P.M. was supported by the ASR/DOE program under DE-SC0000991/003 and the NASA MAPS Program. J. Mayer, E. Fitzgerald, D. Collins, and J. Cahill provided assistance with UCSD/SIO equipment setup. The authors gratefully acknowledge the NOAA Air Resources Laboratory (ARL) for the provision of the HYSPLIT transport and dispersion model and READY website (www.arl.noaa.gov/ready.php) used in this publication and the Office of Naval Research for provision of NAAPS data. J. Ayers and R. Palikonda (Science Systems and Applications) provided GOES-11 cloud top heights used for HYSPLIT back trajectory analysis and %Ice in cloud. The deployment of the NOAA and UCSD/SIO equipment at the Sugar Pine site involved many field staff, particularly C. King (NOAA/ESRL/PSD). The deployment of the DOE Gulfstream-1 involved many PNNL/Atmospheric Radiation Measurement field staff, particularly E. Dukes, J. Hubbe, C. Kluzek, H. Jonsson, M. Pekour, and B. Schmid. M. Hubbell and B. Svancara flew the G-1 for the CalWater flight campaign. D. Collins and R. Spackman provided insightful discussions during the editing stages of this manuscript. T. Lersch of R. J. Lee provided TEM analyses of collected IN. Data available in this paper are available in the supplementary materials.

Supplementary Materials
www.sciencemag.org/cgi/content/full/science.1227279/DC1
Materials and Methods
Supplementary Text
Figs. S1 to S15
Tables S1 to S3
References

11 July 2012; accepted 6 February 2013
Published online 28 February 2013;
10.1126/science.1227279

Multiple Instances of Ancient Balancing Selection Shared Between Humans and Chimpanzees

Ellen M. Leffler,[1]*† Ziyue Gao,[2]* Susanne Pfeifer,[3]* Laure Ségurel,[1,4]* Adam Auton,[5]‡ Oliver Venn,[5] Rory Bowden,[3,5] Ronald Bontrop,[6] Jeffrey D. Wall,[7] Guy Sella,[8,9] Peter Donnelly,[3,5] Gilean McVean,[3,5]§ Molly Przeworski[1,4,8]†§

Instances in which natural selection maintains genetic variation in a population over millions of years are thought to be extremely rare. We conducted a genome-wide scan for long-lived balancing selection by looking for combinations of SNPs shared between humans and chimpanzees. In addition to the major histocompatibility complex, we identified 125 regions in which the same haplotypes are segregating in the two species, all but two of which are noncoding. In six cases, there is evidence for an ancestral polymorphism that persisted to the present in humans and chimpanzees. Regions with shared haplotypes are significantly enriched for membrane glycoproteins, and a similar trend is seen among shared coding polymorphisms. These findings indicate that ancient balancing selection has shaped human variation and point to genes involved in host-pathogen interactions as common targets.

Balancing selection is a mode of adaptation that leads to the persistence of variation in a population or species in the face of stochastic loss by genetic drift. In humans, examples include the sickle cell hemoglobin polymorphism, maintained by heterozygote advantage in environments in which *Plasmodium falciparum* is endemic, as well as other cases that likely arose recently in evolution in response to malaria (*1*). Beyond humans, examples of balancing selection are known in a wide range of organisms and often seem to arise from predator-prey or host-pathogen interactions (*2*–*8*). Most are not thought to be due to heterozygote advantage but to negative frequency-dependent selection, as occurs at self-incompatibility loci in plants (*5*, *9*), or to temporally or spatially varying selection, as seen at R genes in *Arabidopsis*, for example (*4*). The genetic basis is known only in a small subset of cases, however, and the age-old question (*10*–*12*) of how much genetic variation is maintained by balancing selection remains largely open.

When balancing selection pressures result in the stable maintenance of genetic variation in the population for long periods of time, neutral diversity accumulates at nearby sites; in other words, ancient balancing selection leads to deep coalescence times to a common ancestor at the selected site (or sites) and closely linked ones (*13*). One approach to identify targets is therefore to scan the genome for regions of high diversity or other related features, such as intermediate allele frequencies (*14*). A challenge is that such patterns of diversity can occur by chance because of the tremendous variance in coalescence times due to genetic drift alone (*14*). As an illustration, under a simple demographic model with no selection, the probability that two human lineages do not coalesce before the split with chimpanzee is on the order of 10^{-4} (*15*, *16*). Although this probability is small, the human genome is large, and so many such regions could occur by chance. To circumvent this difficulty, we looked for cases in which an ancestral polymorphism has persisted to the present time in both humans and chimpanzees, that is, is shared identical by descent between the two species. This outcome is not expected to occur by genetic drift alone because it requires that neither human nor chimpanzee lineages coalesce before the human-chimpanzee ancestor, which is unlikely even in a large genome (*16*).

To date, two cases of human polymorphisms shared with other apes have been shown to be identical by descent [additional background is available in fig. S1 and (*16*)]: variants in the major histocompatibility complex (MHC), a complex encoding cell surface glycoproteins that present peptides to T cells (*17*), and polymorphisms at ABO, a glycosyltransferase, that underlie the A and B blood groups (*18*). Ancient balancing selection leaves a narrow footprint in genetic variation (*15*, *18*), however, which may be particularly difficult to detect without dense variation data (*19*). Thus, the recent availability of genome sequences for multiple humans and chimpanzees provides an opportunity to search comprehensively and with greater power for ancient balancing selection.

Identification of shared SNPs and haplotypes. We examined complete genome sequences from 59 humans from sub-Saharan Africa (Yoruba) (*20*) and 10 Western chimpanzees (*Pan troglodytes verus*) (*21*) in order to identify shared polymorphisms—namely, high-quality orthologous SNPs with identical alleles in the two species (table S1) (*16*). In total, 33,906 autosomal and 492 X-linked single-nucleotide polymorphisms (SNPs) passed our filters (table S2). The lower proportion of shared SNPs found on the X (in humans, 0.36% of autosomal SNPs versus 0.19% of X-linked

[1]Department of Human Genetics, 920 E 58th Street, University of Chicago, Chicago, IL 60637, USA. [2]Committee on Genetics, Genomics and Systems Biology, University of Chicago, Chicago, IL 60637, USA. [3]Department of Statistics, 1 South Parks Road, University of Oxford, Oxford OX1 3TG, UK. [4]Howard Hughes Medical Institute, University of Chicago, Chicago, IL 60637, USA. [5]Wellcome Trust Centre for Human Genetics, Roosevelt Drive, Oxford OX3 7BN, UK. [6]Department of Comparative Genetics and Refinement, Biomedical Primate Research Centre, Lange Kleiweg 139 2288 GJ, Rijswijk, Netherlands. [7]Institute for Human Genetics, University of California, San Francisco, San Francisco, CA 94143, USA. [8]Department of Ecology and Evolution, 1101 E. 57th Street, Chicago, IL 60637, USA. [9]Department of Ecology, Evolution and Behavior, Alexander Silberman Institute of Life Sciences, Hebrew University of Jerusalem, Jerusalem 91904, Israel.

*These authors contributed equally to this work.
†Corresponding author. E-mail: emleffler@uchicago.edu (E.M.L.); mfp@uchicago.edu (M.P.)
‡Present address: Department of Genetics, Albert Einstein College of Medicine, New York, NY 10461, USA
§These authors co-supervised this work.

Downloaded from http://science.sciencemag.org/ on January 21, 2017

EXTENDED PDF FORMAT
SPONSORED BY

www.rndsystems.com

Science
AAAS

Dust and Biological Aerosols from the Sahara and Asia Influence Precipitation in the Western U.S.

Jessie M. Creamean, Kaitlyn J. Suski, Daniel Rosenfeld, Alberto Cazorla, Paul J. DeMott, Ryan C. Sullivan, Allen B. White, F. Martin Ralph, Patrick Minnis, Jennifer M. Comstock, Jason M. Tomlinson and Kimberly A. Prather (February 28, 2013)
Science **339** (6127), 1572-1578. [doi: 10.1126/science.1227279]
originally published online February 28, 2013

Editor's Summary

Action at a Distance

Snowfall in the Sierra Nevada provides a large fraction of the water that California receives as precipitation. Knowing what factors influence the amount of snow that falls is thus critical for projecting how water availability may change in the future. Aerosols have an important effect on cloud processes and precipitation. **Creamean *et al.*** (p. 1572, published online 28 February) found that dust and biological aerosols originating from as far away as the Sahara facilitate ice nuclei formation and ice-induced precipitation in the Sierra Nevada and show how dust and biological articles from places as distant as Africa and Asia can influence precipitation over the western United States.

This copy is for your personal, non-commercial use only.

Article Tools Visit the online version of this article to access the personalization and article tools:
http://science.sciencemag.org/content/339/6127/1572

Permissions Obtain information about reproducing this article:
http://www.sciencemag.org/about/permissions.dtl

Science (print ISSN 0036-8075; online ISSN 1095-9203) is published weekly, except the last week in December, by the American Association for the Advancement of Science, 1200 New York Avenue NW, Washington, DC 20005. Copyright 2016 by the American Association for the Advancement of Science; all rights reserved. The title *Science* is a registered trademark of AAAS.

Downloaded from http://science.sciencemag.org/ on January 21, 2017